Geometallurgical domain characterisation and process performance prediction for ferromanganese ores from the Paling Pan MnFe deposit, Postmasburg Manganese Field, South Africa

by M. Buthelezi[1], G.T. Nwaila[1], D. Bussin[2,3], A.J.B. Smith[2,3], C. Vorster[2,3], G.M. Bybee[1], M.S.D. Manzi[1]

Affiliation:
1 African Research Centre for Ore Systems Science (CORES), School of Geosciences, University of the Witwatersrand, South Africa
2 Paleoproterozoic Mineralisation (PPM) Research Group, Department of Geology, University of Johannesburg, South Africa
3 Department of Science and Innovation-National Research Foundation Centre of Excellence in Mineral and Energy Resource Analysis, Department of Geology, University of Johannesburg, South Africa

Correspondence to:
M. Buthelezi

Email:
musawenkosi.buthelezi@students.wits.ac.za

Dates:
Received: 30 Jan. 2026
Revised: 25 Aug. 2026
Accepted: 02 Oct. 2026
Published: Oct. 2026

How to cite:
Buthelezi M., Nwaila G.T., Bussin D. Smith A.J.B., Vorster C., Bybee G.M., Manzi M.S.D. 2026. Geometallurgical domain characterisation and process performance prediction for ferromanganese ores from the Paling Pan MnFe deposit, Postmasburg Manganese Field, South Africa . *Journal of the Southern African Institute of Mining and Metallurgy*, vol. 126, no. 10, pp. 597 – 606

DOI ID:
https://doi.org/10.17159/2411-9717/3899/2026

ORCiD:
M. Buthelezi
https://orcid.org/0000-0003-2704-9317
G.T. Nwaila
https://orcid.org/0000-0002-3974-9890
D. Bussin
https://orcid.org/0000-0002-4747-6765
C. Vorster
https://orcid.org/0000-0003-0514-2991
G.M. Bybee
https://orcid.org/0000-0002-3156-551X
M.S.D. Manzi
https://orcid.org/0000-0002-1654-5211

Abstract

Manganese is a critical metal for the global steel industry, with South Africa as the leading producer of Mn ore. Efficient processing of its complex ores, particularly those in the Postmasburg Manganese Field, requires site-specific understanding of their variability. This study develops a geometallurgical framework for the Paling Pan Fe-Mn deposit, integrating mineralogy, geochemistry, and quantified ore texture to define domains that predict processing performance. Four principal ore textures, those being, massive, vuggy, layered, and conglomeritic, were characterised, each influencing beneficiation differently. A dataset of 256 samples was used to train predictive machine learning (XGBoost) models for magnetic separation and dense media separation. Incorporating texture-differentiated domains improved prediction accuracy, particularly for dense media separation yield (2.6% increase in chemical oxygen demand). Magnetic separation yields ranged from 72.3% to 92.3%, with massive ores performing best. SHAP analysis identified manganese grade, Fe grade, and ore texture as critical predictors for magnetic separation, while specific gravity and gangue content dominated dense media separation performance. This integrated, data-driven approach provides a robust methodology for optimising plant design, ore blending, and processing strategies, enhancing resource efficiency, economic viability, and sustainability in manganese ore exploitation.

Keywords

geometallurgy, manganese ores, magnetic separation, dense media separation, XGBoost, process optimisation, Postmasburg Manganese Field

Introduction

Manganese (Mn) is critical for the global industry, primarily in steel manufacturing but also in aluminium alloys and battery components (Habashi, 2008; Sun et al., 2020; Song et al., 2023). South Africa is the major global producer of Mn ore, underscoring the importance of understanding its deposits for optimal extraction (Von der Heyden et al., 2024). Current research in geometallurgy examines the interplay between ore grade, mineralogy, and processing efficiency, with ore texture being a crucial but often qualitative variable. Despite its recognised importance, ore texture is rarely quantified or operationalised within geometallurgical predictive models for Mn deposits.

The Paling Pan Fe-Mn deposit is located in the western belt of the Postmasburg Manganese Field (PMF) (Figure 1). The deposit is characterised by significant heterogeneity in ore characteristics. Previous studies have documented a variety of ore textures, including massive, vuggy, layered, and conglomeritic types, in the western belt of the PMF and at Paling Pan (Gutzmer, Beukes, 1996; Bussin, 2022). This textural variability presents a substantial challenge for achieving consistent processing performance and accurate grade prediction. While the mineralogy, dominated by braunite and bixbyite with gangue minerals such as kaolinite, diaspore, and hematite, is well-understood, the quantitative association between ore texture and processing response remains inadequately explored. This study bridges this gap by integrating detailed geological logging, geochemical analysis, and machine learning (ML) to objectively classify ore textures and predict key processing performance indicators. We adopt a narrow, process-facing definition of geometallurgy, where the primary value of geological attributes

lies in their ability to predict plant responses such as recovery, product quality, and energy consumption (Lishchuk et al., 2015). Consequently, we define ore texture as a key geological driver and quantify its impact, integrating it with chemistry and ML into a deployable domaining protocol for the Paling Pan deposit. This study is a companion study to Buthelezi et al. (2026), who examined ML-based classification of ore textures and MnO grade prediction at the same deposit. While the previous study focused on geological characterisation, the present work addresses a distinct metallurgical objective: the definition of geometallurgical domains and the prediction of processing performance for magnetic separation and dense media separation.

Geological setting

Regional context

The Paling Pan Fe-Mn deposit is situated within the PMF, with the latter located in the centre of the Maremane dome anticline between the towns of Postmasburg and Sishen in the Northern Cape Province of South Africa (Figure 1) (Smith, Beukes, 2016). The PMF extends along a north-south strike of approximately 65 km. The mineralisation within the PMF occurs at the contact between the approximately 2.5 Ga Campbellrand Subgroup carbonates of the Griqualand West region of the Transvaal Supergroup and the approximately 2.0 Ga pre-Gamagara erosional unconformity (Gutzmer, Beukes, 1996; Beukes et al., 2016; Smith, Beukes, 2016).

Paling Pan Fe-Mn ore deposit

In this contribution, detailed stratigraphic and mineralogical descriptions of the Paling Pan Fe–Mn deposit are not reproduced in full; instead, the reader is referred to the Supplementary Data files archived in the South African Journal of Geology repository (Buthelezi et al., 2026). To avoid duplicating this material and to prevent plagiarism, only a summary is provided here. The supplementary files document the drill-core-defined succession from the Campbellrand dolostone footwall through the lower wad unit and principal mineralised zone to the Doornfontein Member conglomerate and overlying Doornfontein and Sishen shales (Figure 2), as well as the ore textures, thickness ranges, and genetic interpretation of Gutzmer and Beukes (1996) and Bussin (2022).

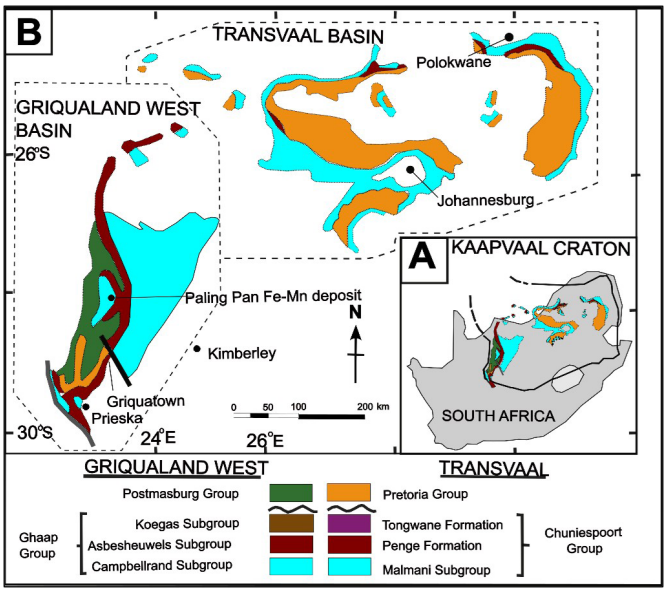


Figure 1—Simplified geological map showing (a) the location of the Transvaal Supergroup in South Africa and (b) the approximate position of the Paling Pan deposit within the Griqualand West Basin (modified after Warke, 2016; Buthelezi et al., 2026)

Data and analytical methods

Datasets

The dataset for this study was sourced from Bussin (2022) and comprises 256 lithogeochemical samples (ore zones) collected from 36 drill cores in the Paling Pan Fe-Mn deposit. Textures were defined through systematic megascopic logging of drill cores. For each of the 256 analysed samples, clast size and support, visible porosity, and density/consolidation were recorded semi-quantitatively, and representative samples were verified using a hand lens and, where necessary, petrographic examination. The samples fall into four textural classes: conglomeratic (n = 100, 39.1%), layered (n = 68, 26.6%), massive (n = 67, 26.2%), and vuggy (n = 21, 8.2%).

Sampling was not initially uniform, as secondary targets were selected based on field observations. This selective sampling approach introduces a degree of human bias and imposes certain limitations on the dataset, particularly in the representation of textural transitions and lower-grade zones. Therefore, the findings should be interpreted as characteristic of mineralised zones rather than averages for the entire deposit. Lithogeochemical analyses were conducted using X-ray fluorescence (XRF) spectrometry on borate fusion discs at SGS Laboratories in Johannesburg, employing a Malvern Analytic WD-XRF instrument. The major oxide components analysed included Al_2O_3, CaO, Fe_2O_3, K_2O, Na_2O, P_2O_5, SiO_2, TiO_2, MnO, V_2O_5, and BaO, with results expressed in weight percent (wt.%). The machine learning (ML) workflow requires complete training features but not prediction targets. Therefore, missing compositions, which are only in NaO (n = 2; 0.008 % of the dataset), are imputed using the k-nearest neighbours' algorithm (Hron et al., 2010). The analytical error for most elements is less than 0.01%, except for P2O5, which has an error of 0.002%, as indicated in an unpublished SGS laboratory certificate and documented by Bussin (2022).

Evaluation of the beneficiation response of the Paling ferromanganese deposit was conducted via multi-stage Permroll

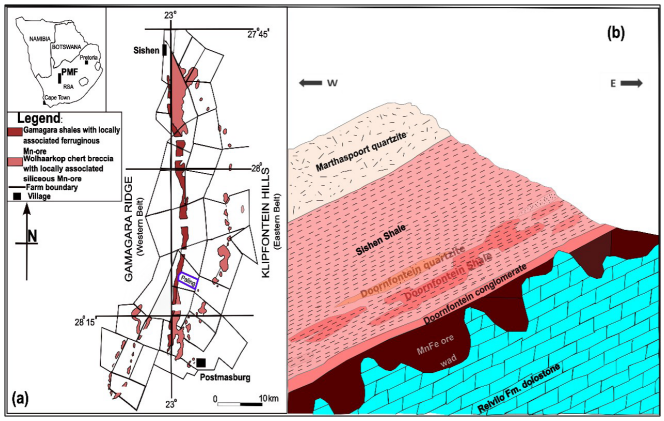


Figure 2—Regional map of the PMF showing the distribution of Gamagara (Mapedi formation) shales associated with Fe-Mn ore (Western Belt) and the location of the Paling Pan Exploration area in relation to Postmasburg and Sishen; (b) schematic stratigraphic section at the Paling Pan deposit (modified after Gutzmer, Beukes,1996; Bussin, 2022; Buthelezi et al., 2026)

magnetic separation on six 2.5 kg composite samples compiled from 42 representative reverse circulation (RC) drill chip intervals across seven boreholes12. To standardise test feed kinetics, samples were homogenised using a two-tier riffle splitter and screened to an intermediate > 1 mm to < 5.6 mm size fraction prior to sequential pass-through over barium ferrite (BaFe; 2,000 Gauss), samarium cobalt (SmCo; 4,000 Gauss), and neodymium (Nd; 7,000 Gauss) permanent magnetic rollers at MINTEK. Products comprising rougher, scavenger 1, scavenger 2 concentrates, and final tailings were pulverised at the University of Johannesburg for major-element borate-fusion XRF spectrometry at SGS Randfontein and quantitative X-ray diffraction (XRD) phase analysis at SPECTRUM. Pre-screening of the test feed removed the < 1 mm fines, which selectively discarded soft kaolinite gangue and artificially elevated measured feed grades relative to field estimates.

Furthermore, testing on fine particle sizes (> 1 mm to < 5.6 mm) introduces significant particle-size liberation bias when extrapolated to standard lump manganese market specifications (+42 mm). Dataset fidelity was further compromised by the exclusion of non-ore lithologies inevitably incorporated during open-pit mining cuts (e.g., soft shale partings, wad, and dolostone), analytical errors in XRD quantification arising from preferred orientation of platy clay minerals and solid-solution stoichiometry in the (Fe, Mn)$_2O_3$ series, and the necessary rejection of preliminary geochemical data produced by unaccredited analytical facilities (Bussin, 2022).

Methodology for geometallurgical domain definition and modelling

The core of this study involved a multi-stage methodology to define geometallurgical domains and build predictive models. Thresholds for domain definition were selected based on plant operational specifications and historical grade control criteria. First, initial domains were established using chemical thresholds relevant to processing performance. These chemical domains were then enhanced by integrating the four primary ore textures (massive, vuggy, layered, and conglomeritic), creating composite domains such as high-Mn massive and mixed-chemistry conglomeritic.

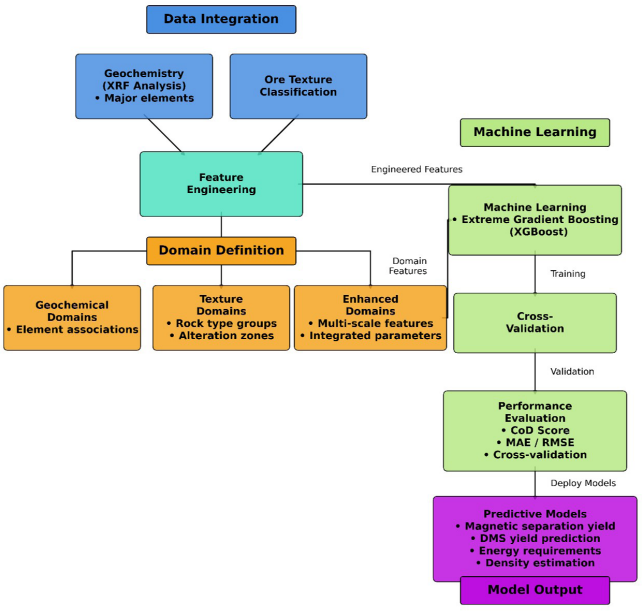


Figure 3—Flowchart illustrating the data integration and ML workflow used in the study

Subsequently, a comprehensive feature engineering step was undertaken to prepare the data for ML, which included the creation of distinct predictor variables. Ore texture and the engineered composite geometallurgical domains (e.g., 'high Mn massive') were treated as nominal categorical features. Both were one-hot encoded. This avoids imposing an arbitrary order on the texture categories and is appropriate because the composite domains have low cardinality (twenty categories). No integer or target encoding was used. All encoding, imputation, and scaling were performed inside each cross-validation fold using a scikit-learn pipeline, so no information from the held-out fold influenced the training data. This eliminates the target leakage that would occur if domain-level averages were computed across the full dataset before cross-validation. Additionally, key geochemical features were derived, including converting MnO and Fe_2O_3 to elemental Mn and Fe grades, deriving phosphorus content from P_2O_5, and calculating a total gangue index as $SiO_2 + Al_2O_3$.

For model development, the XGBoost Regressor algorithm was selected due to its proven performance with tabular data and ability to handle complex, non-linear relationships (Sun et al., 2023). The modelling approach compared three scenarios to quantify the value of domain information: (1) a baseline model with no domain information, (2) a model with simple chemical domains, and (3) a model with the enhanced texture-differentiated domains. Hyperparameter tuning was performed using a randomised search with 5-fold grouped cross-validation by drill hole. All samples from a given drill hole were assigned to the same fold, so no drill hole appeared in both training and validation sets. This prevents spatial similarity between samples from the same drill hole from inflating performance estimates. Random 5-fold cross-validation was also run for comparison; it produced higher R^2 values (e.g., X vs. Y), confirming that the grouped approach gives a more conservative and realistic assessment of performance on unseen parts of the deposit (Figure 3).

Performance evaluation metrics

We evaluate the performance of our models using standard metrics suitable for regression tasks. Model performance was rigorously evaluated using 5-fold cross-validation, and we employed the coefficient of determination, *CoD,* the mean absolute error (MAE), and the root mean squared error (RMSE). The CoD value is computed as

$$CoD = 1 - \frac{\sum_{i=1}^{n}(\hat{Y}_i - \bar{Y})^2}{\sum_{i=1}^{n}(Y_i - Y)^2}, \quad [1]$$

where Y_i are the observed values, $\hat{Y}i$ are the predicted values, and $\bar{Y}$ is the mean of the observed values. A *CoD* value of 1 indicates a perfect prediction, while negative values suggest that the model performs worse than a simple mean prediction (Nagelkerke, 1991; Draper, Smith, 1998). The mean absolute error (MAE) is given by

$$\text{MAE} = \frac{1}{n}\sum_{i=1}^{n}|Y_i - \hat{Y}_i|, \quad [2]$$

which measures the average absolute difference between the observed and predicted values. These metrics enable us to assess the overall fit of the regression model, as well as the average magnitude of the prediction errors, thereby providing a clear picture of model performance (Willmott, Matsuura, 2005).

The RMSE is computed as

$$RMSE = \sqrt{\frac{\sum_{i=1}^{N}(y_i - \hat{y}_i)^2}{N}}, \quad [3]$$

where Y_i are the observed values, $\hat{Y}_i$ are the predicted values, and N is the total number of observations. The RMSE represents the standard deviation of the prediction errors, with a lower value indicating better model accuracy as it signifies smaller average deviations between predicted and observed values (Chai, Draxler, 2014).

SHapley Additive exPlanations (SHAP)

The application of SHapley Additive exPlanations (SHAP) provides a robust framework for quantifying individual predictor contributions in our ML models, offering both global and local interpretability (Lundberg, Lee, 2017). SHAP values provide a theoretically consistent way to attribute model predictions to individual features. The method is based on cooperative game theory, where each feature acts as a player, and its contribution is its average marginal effect across all possible combinations of features. This gives a fair distribution of credit for the prediction. SHAP satisfies three key properties: local accuracy, meaning the sum of feature contributions equals the prediction minus the average prediction; missingness, meaning features with no effect receive zero credit; and consistency, meaning if a feature becomes more important in a new model, its SHAP value does not decrease. These properties make SHAP attributions reliable and comparable across models. The SHAP explanation model takes the form:

$$g(z') = \emptyset_0 + \sum_{i=1}^{M} \emptyset_i z'_i \quad [4]$$

Where $\emptyset_i$ represents the Shapley value for feature *I*, M denotes the total number of features, and $z' \in \{0,1\}^M$ indicates the presence of simplified input features. The exact computation of $\emptyset_i$ is given by:

$$\emptyset_i(f,x) = \sum_{z' \subseteq x'} \frac{|z'|!(M-|z'|-1)!}{M!} [f_x(z') - f_x(z' \backslash i)] \quad [5]$$

This formulation ensures that each feature's contribution reflects its marginal impact across all possible feature permutations (Lundberg, Lee, 2017). This enables us to move beyond a "black box" model and understand which geological and chemical features drive the predictions for magnetic separation and dense media separation (DMS) performance.

Results and discussions

Geometallurgical domain characterisation

Application of the enhanced domaining protocol at the Paling Pan Fe–Mn deposit delineated twenty geometallurgical domains, capturing the heterogeneity of the orebody (Figure 4). The most prevalent domain is mixed chemistry conglomeritic, representing 28.5% of samples (n = 73), followed by high Mn massive (13.3%, n = 34) and high Mn layered (9.4%, n = 24). Additional domains include mixed chemistry layered, mixed chemistry massive, high Mn vuggy, medium Mn (30 wt.%– 35 wt.%) subtypes across layered, massive, conglomeritic, and vuggy textures, low Mn (28 wt.% – 30 wt.%) layered, massive, and conglomeritic domains, as well as high Mn conglomeritic, mixed chemistry vuggy, and a distinct high Fe conglomeritic domain. This distribution mirrors field observations, where conglomeritic and layered textures are widespread and associated with complex mineralogy typical of karst-hosted manganese deposits (Gutzmer, Beukes, 1996; Tsikos et al., 2003). Classification was based on Mn thresholds: high Mn (> 40 wt.%), medium Mn (25 wt.% –3 5 wt.%), and low grade (< 25 wt.%). The chemical signatures of each domain, including systematic variations in Fe, Al_2O_3, and SiO_2 are illustrated in Figures 4a and b, highlighting distinct compositional trends across the deposit.

Processing performance by domain

The magnetic separation test work conducted using a multi-stage permanent roll (Permroll) apparatus at intensities of 2000, 4000, and 7000 Gauss revealed clear domain-specific performance trends. The results from the simple geochemistry-based domains (Figure 5a) show a strong correlation between MnO grade and mass recovery. The cumulative mass recovery in the magnetic concentrates varied significantly, with the highest yield of 92.3% achieved for the high-grade Mn (> 32%) domain, followed by 90.3% for the Mn (> 40%) domain. In contrast, the lower-grade Mn (> 28%) domain showed a substantially lower recovery of 72.3%. This performance hierarchy is consistent with the defined geometallurgical domains in the reference values, confirming that domains exceeding the Mn > 32% threshold deliver optimal magnetic separation yields.

This trend is further refined in the ore texture-based domains (Figure 5b), which integrates geochemistry with mineralogical texture for the top eight domains. The enhanced predictive capability of this model explains the mineralogical observation that the strong magnetic response of bixbyite, effectively concentrated in the rougher and scavenger 1 stages, drives the high recoveries in Mn-rich domains. Although hematite's weaker magnetic susceptibility typically causes it to report to the non-magnetic fraction at standard intensities (Elliott, Barati, 2020), it becomes magnetically susceptible at high field strengths. This explains the significant increase of hematite in the magnetic concentrate (scavenger 2) and the corresponding decrease in Mn grade observed in this study. The integration of texture in Figure 5b, thus provides a more robust framework for predicting processing performance, moving beyond simple chemical composition to account for the textural associations that ultimately control separation efficiency during both magnetic separation and DMS processes.

The ore texture proved to be a critical factor influencing processing efficiency. Massive ores, with their dense and homogeneous nature, consistently delivered superior outcomes, averaging a magnetic yield of 80.4%, a DMS yield of 85.1%, and a high-density profile (~3.6 g/cm³ × 20; Figure 5b). In contrast, vuggy ores, characterised by porosity and heterogeneous mineral distribution, exhibited lower and more variable performance, with average magnetic and DMS yields of 73.0% and 72.8%, respectively, and reduced density (~3.2 g/cm³ × 20). This link between texture, mineral liberation, and density highlights ore texture as a primary source of processing variability (Parian et al., 2017).

Machine learning model performance

The comparative analysis of the three ML feature-set schemes (no_domain, simple_domain, enhanced_domain) demonstrates the tangible value of incorporating texture-differentiated domains. Across both by-drillhole and random validation schemes, performance differences were consistent but nuanced. For magnetic separation yield, the enhanced_domain achieved strong results (CoD) ≈ 0.811 by-drillhole, 0.839 random), though the no_domain baseline remained competitive (CoD ≈ 0.817 and 0.840, respectively). Error metrics (MAE, RMSE) were lowest for no_ domain under random splits, but the enhanced domain maintained comparable precision, underscoring that textural information contributes explanatory power without sacrificing stability. For estimated density, improvements were marginal across all schemes. CoD values clustered tightly (0.752 – 0.760 by-drillhole; 0.777 –

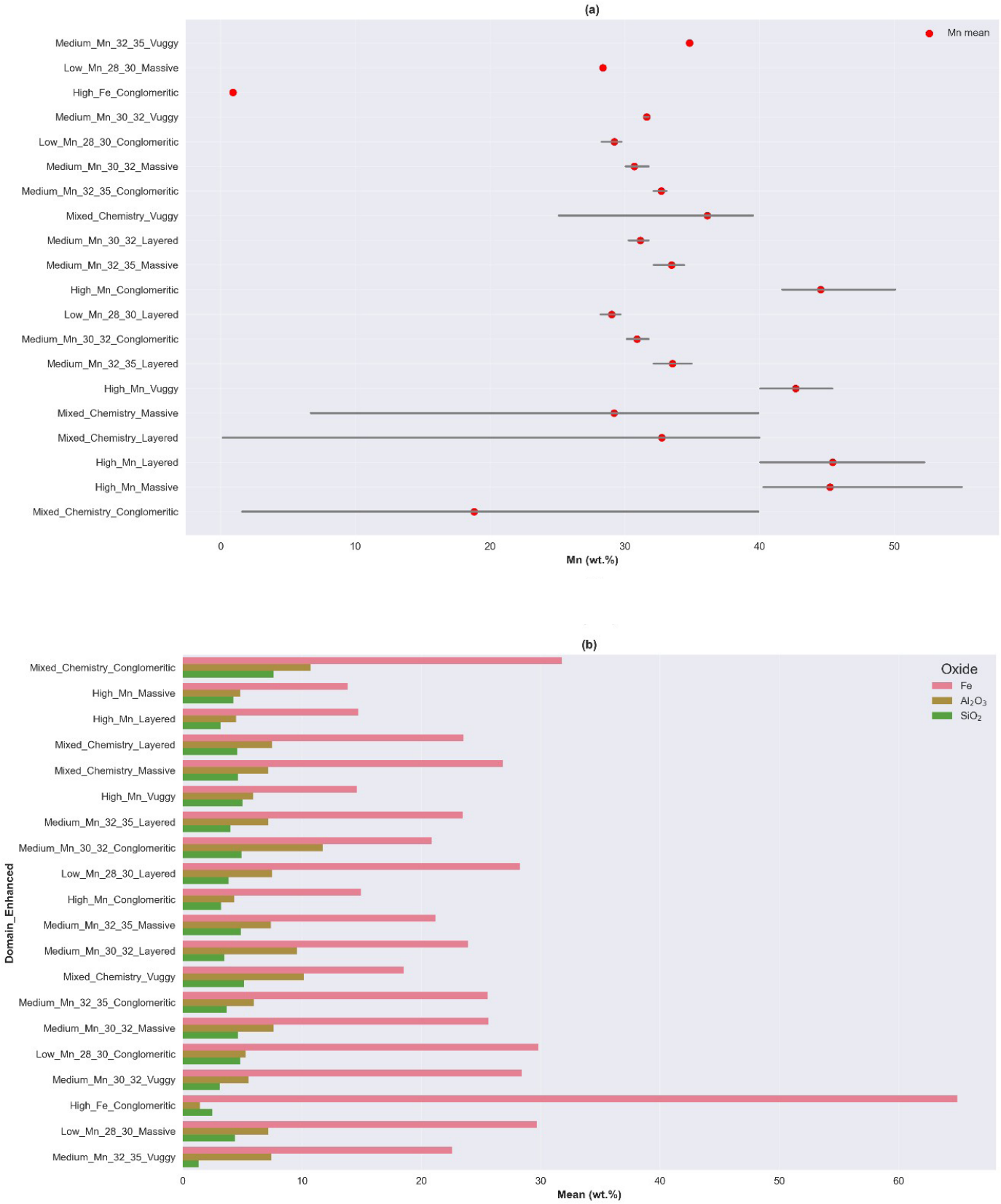


Figure 4—Geometallurgical domain characterisation of the Paling Pan Fe-Mn deposit. (a) Range and mean values of Mn (wt.%) across geochemical domains. Horizontal bars represent the minimum–maximum range, while red markers indicate the mean concentration. (b) Average concentrations of Fe, Al_2O_3, and SiO_2 (wt.%) for each domain. The bar plot highlights compositional variations among ore textures, illustrating differences in oxide abundances across sampled domains

Geometallurgical domain characterisation and process performance prediction

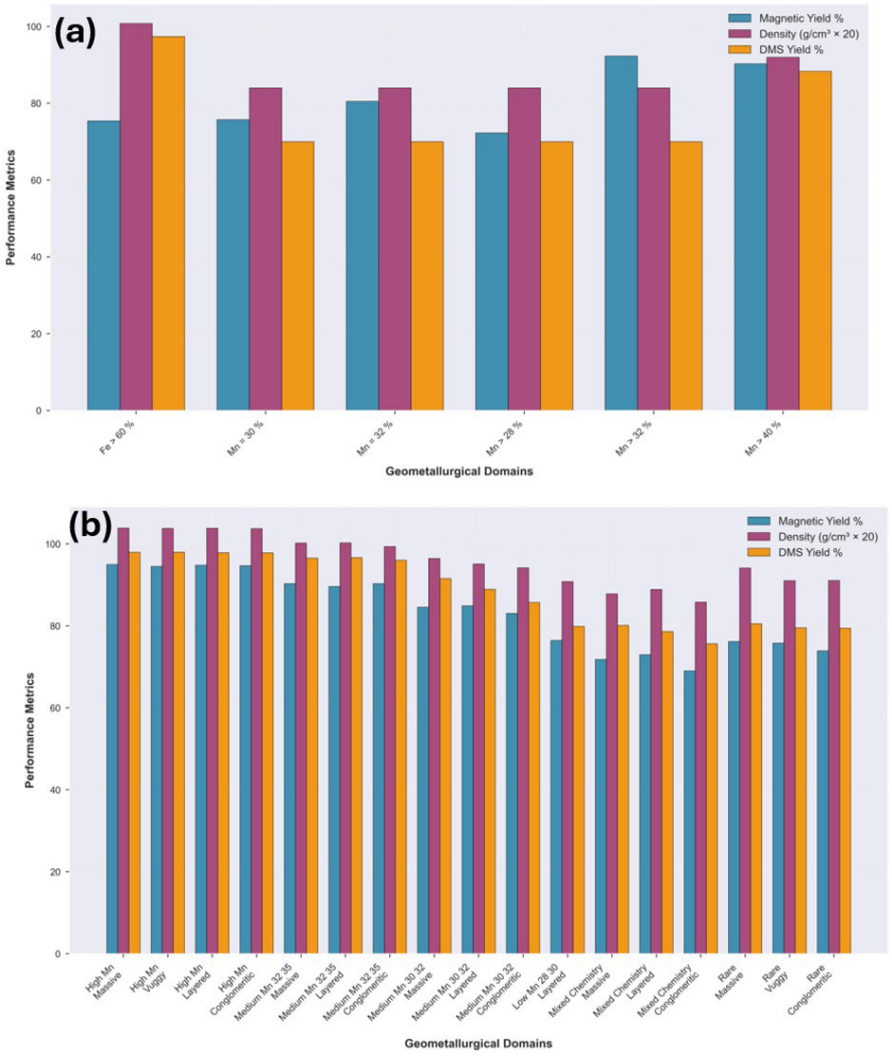


Figure 5—Predicting Fe-Mn processing performance from geometallurgical properties (magnetic separation, density, DMS) at the Paling Pan Fe-Mn ore deposit. (a) Simple domains based solely on geochemistry. (b) Ore texture-based domains, including geochemistry for the top 8 domains

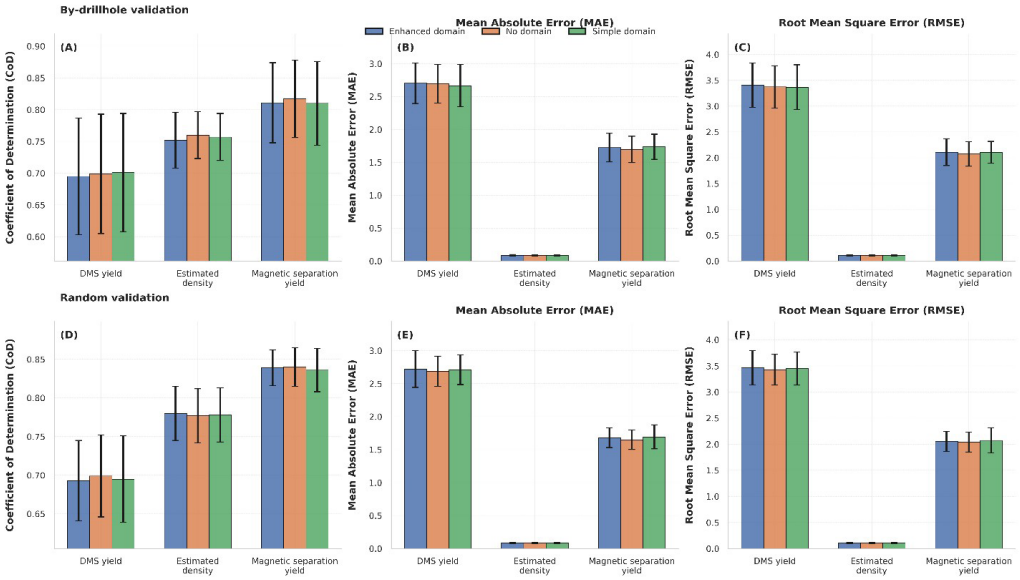


Figure 6—Performance of machine-learning models across three domain feature sets (enhanced domain, no domain, simple domain) under two validation schemes (by-drillhole and random). Each panel presents mean values with standard deviation error bars for three predictive targets, DMS yield, estimated density, and magnetic separation yield, evaluated using the CoD, MAE, and RMSE. The plots highlight how domain incorporation influences predictive accuracy and precision, with texture-differentiated domains yielding notable improvements in recovery predictions

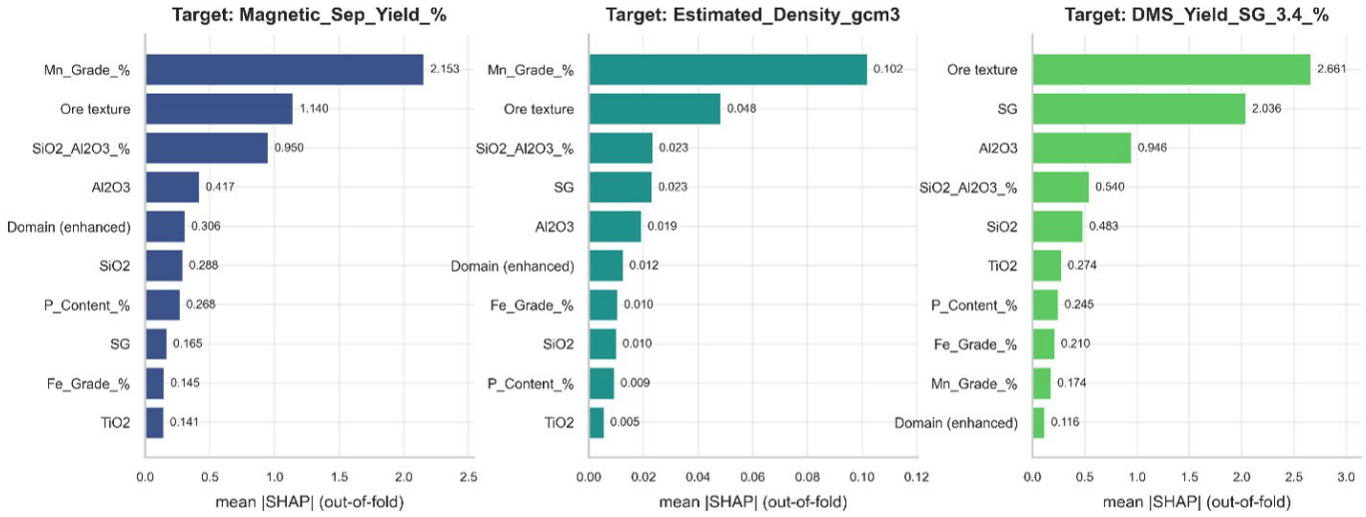


Figure 7—Comparative feature importance scores from SHAP analysis for XGBoost models predicting three key metallurgical performance indicators: (a) magnetic separation yield, (b) estimated density, and (c) dense media separation yield

0.780 random), with error metrics nearly identical (MAE ≈ 0.087 – 0.089, RMSE ≈ 0.106 – 0.108). This confirms that density prediction is primarily controlled by chemical composition, and domain integration does not materially alter variance explained.

The most significant gains were observed for DMS yield. Under by-drillhole splits, simple_domain achieved the best balance (CoD = 0.701, MAE = 2.667, RMSE = 3.369), while under random splits, no_domain slightly edged CoD (0.699) but with higher errors. The enhanced_domain consistently reduced RMSE relative to baseline (e.g., 3.406 vs. 3.373 by-drillhole; 3.466 vs. 3.428 random), highlighting that textural features improve precision in gravity-based separation predictions. Although CoD improvements are numerically modest, the concurrent reduction in MAE and RMSE is operationally significant. These reductions represent models that are not only more accurate on average but also more precise and reliable (Koch et al., 2019; Tusa et al., 2025). In industrial contexts, even marginal gains in prediction fidelity translate directly into economic value through optimised recovery, reduced energy consumption, and consistent product quality (Figure 6).

Feature importance analysis

The SHAP analysis of feature importance within the XGBoost models provided clear, quantifiable insights into the dominant controls on processing performance. For magnetic separation yield, Mn wt.% was the most influential feature (mean |SHAP| = 2.153), followed by ore texture (1.140) and the composite geometallurgical domain (0.306) (Figure 7a). This confirms that while mineral chemistry exerts primary control, textural attributes and spatial domain context also contribute meaningfully, likely through their influence on mineral liberation during comminution (Lamberg, 2011; Parian et al., 2017).

For estimated density, Mn grade % again dominated (0.102), with ore texture (0.048) and SiO_2–Al_2O_3 wt.% (0.023) providing secondary importance (Figure 7b). Despite measurable textural contributions, domain integration did not improve density prediction performance, indicating that chemical composition remains the stronger determinant of variance. In contrast, for DMS yield, ore texture was overwhelmingly dominant (2.661), followed by SG (2.036) and Al_2O_3 (0.946) (Figure 7c). This underscores that for gravity-based separation, the ore's textural properties and liberation characteristics are critical, as efficiency is highly sensitive to particle size, shape, and porosity (Napier-Munn, 2015; Wills, Finch, 2015).

Geometallurgical Implications

The geometallurgical domain classification and predictive models developed in this study provide a critical, data-driven framework for optimising the entire mining value chain of ferromanganese ores within the Paling Pan Fe-Mn deposit. The transition from a traditional, chemically focused resource model to an advanced mineralogical approach enables a spatially-based predictive model essential for modern production management (Lamberg, 2011). This framework has direct and actionable implications for mine planning, process optimisation, resource efficiency, and exploration strategy, which are of significant relevance to the Southern African mining context.

The primary implication lies in enabling predictive mine planning and intelligent ore blending. By integrating the geometallurgical domains, defined by both modal geochemistry and ore texture, into the resource block model, mine planning evolves from a geometric exercise to a metallurgically-informed strategy. This allows for strategic sequencing and blending to ensure a consistent plant feed, directly mitigating the operational disruptions and recovery losses caused by unforeseen variations in ore hardness and mineral liberation characteristics (Lamberg, 2011; Lund et al., 2013; Lishchuk et al., 2015).

The study also demonstrates potential for pre-emptive process design and dynamic optimisation. Predictive ML models using texture and geochemistry to forecast comminution energy and liberation yield enable a shift from reactive to pre-emptive processing. This facilitates domain-specific routing within the plant (Hunt et al., 2013; Parian, 2017; Dominy et al., 2018). For example, high-yield massive ores can be directed to simple magnetic circuits, while conglomeritic ores, where liberation is more challenging, are managed with flexible, multi-stage routes designed for higher

recovery. This aligns with deeper levels of geometallurgical implementation, where process changes are planned based on forecasted feed quality (Lamberg et al., 2011; Lindberg, 2013; Lishchuk et al., 2015).

Another advantage of the geochemistry-aware approach relates to the oxidation state of Mn in the final ore product delivered to the Mn smelters that produce ferromanganese and silicomanganese for steelmaking. The Mn minerals in the ore needs to be reduced by coke in this process, with the energy required to do this varying between the different Mn ore minerals because of different Mn^{2}+, Mn^{3}+ and Mn^{4}+ contents, with energy requirement increasing as the oxidation state increases (Cairncross, Beukes, 2013; Von der Heyden et al., 2024). Better modelling of the relative abundances of Mn minerals in the different domains can therefore inform Mn smelters of the energy requirements of their processes depending on variations in the ore feed.

A significant implication for sustainable resource development is enhanced resource efficiency and reduced environmental liability. While this study did not demonstrate reductions in ore-waste misclassification, other work has shown that predictive geometallurgical models can reduce misclassification and improve resource utilisation (Abdolmaleki et al., 2025). Extending this framework with more mineralogical data could form future work to achieve similar outcomes. By accurately forecasting in situ processing yield, such models can maximise resource utilisation, extend mine life, and reduce environmental footprint by lowering waste rock and tailings volumes (Lishchuk, 2016). This supports industry goals of improved environmental, social, and governance (ESG) performance.

Finally, the methodology provides a foundation for value-driven, data-led exploration. Applying this texture-aware, geochemistry-based framework early in the project lifecycle allows exploration to be targeted not only towards geological tonnage but towards economic tonnage with favourable processing characteristics. As demonstrated at the Kemi chromite mine, systematic grain size measurement was used for recovery forecasts (Lishchuk et al., 2015). Similarly, future integration of mineralogical datasets with textural and geochemical predictors could de-risk exploration projects and prioritise domains with superior potential returns, a critical strategic consideration for long-term viability in the Southern African mining context.

Conclusion

This study demonstrates that integrating ore texture into geometallurgical domain classification significantly improves the prediction of processing performance for ferromanganese ores at the Paling Pan deposit. While chemistry remains the primary control on density, textural attributes strongly influence recovery in magnetic and gravity-based separation, with massive ores consistently outperforming vuggy and conglomeritic types. The machine learning models, supported by SHAP analysis, highlight Mn wt.%, Fe wt.%, and ore texture as key drivers of beneficiation outcomes, confirming the operational importance of texture in recovery variability. These findings have direct implications for predictive mine planning, intelligent ore blending, and process optimisation, enabling more consistent plant performance and reduced operational risk. Beyond immediate processing benefits, the framework also informs smelter energy requirements by modelling Mn oxidation states, thereby contributing to sustainable resource efficiency. Overall, the integration of geochemistry, ore texture, and machine learning establishes a deployable geometallurgical protocol that enhances economic viability, supports environmentally responsible mining, and provides a strategic advantage for the long-term exploitation of manganese resources in South Africa.

Acknowledgements

The authors acknowledge the support provided by 4Arrows Mining and Exploration and PMG Mining (Pty) Ltd for access to the processing data and samples used in this study. Special thanks to SGS Laboratories and MINTEK for analytical support. The Department of Science and Technology–National Research Foundation Centre of Excellence in Mineral and Energy Resource Analysis (DSTI-NRF CIMERA) is acknowledged for its financial support.

Credit authorship contribution statement

M. Buthelezi: Conceptualisation, investigation, writing - original draft.

G.T. Nwaila: Software, methodology, writing - review and editing.

D. Bussin: Data curation, investigation.

A.J.B. Smith: Writing - review and editing.

G.M. Bybee: Validation, writing - review and editing.

M.S.D. Manzi: Supervision, project administration, writing - review and editing.

Ethics declarations

Competing financial interests

The author declares that there are no known competing financial interests or personal relationships that could have appeared to influence the work reported in this paper.

References

Abdolmaleki, M., Ghadernejad, S., Esmaeili, K. 2025. Automated Hyperspectral Ore–Waste Discrimination for a Gold Mine: *Comparative Study of Data-Driven and Knowledge-Based Approaches in Laboratory and Field Environments. Minerals*, vol. 15, no. 7, pp.741. https://doi.org/10.3390/min15070741

Beukes, N.J., Swindell, E.P., Wabo, H. 2016. Manganese deposits of Africa. *Episodes Journal of International Geoscience*, vol 39, no. 2, 285-317. https://doi.org/10.18814/epiiugs/2016/v39i2/95779

Buthelezi, M., Nwaila, G.T., Bybee, G.M., Manzi, M.S.D., Bussin, D., Vorster, C., Smith, A.J.B., Kennedy, B. 2026. Predictive modelling of manganese ore textures from a selectively sampled drill core dataset: A case study of the Paling Pan ferruginous manganese deposit, Postmasburg Manganese Field. *South African Journal of Geology*, vol. 129, no. 2, pp. 347–372. https://doi.org/10.25131/sajg.129.2806.sup-mat

Bussin, D. 2022. A Characterisation and Process Mineralogical Assessment of the Karst-Hosted Manganese Ore Deposits at Paling Exploration Camp in the Postmasburg Manganese Field, Northern Cape Province, South Africa. Master's thesis, University of Johannesburg.

Chai, T., Draxler, R.R. 2014. Root mean square error (RMSE) or mean absolute error (MAE)?–Arguments against avoiding RMSE in the literature. *Geoscientific model development*, vol. 7, no. 3, pp. 1247–1250. https://doi.org/10.5194/gmd-7-1247-2014

Dominy, S.C., O'Connor, L., Parbhakar-Fox, A., Glass, H.J., Purevgerel, S. 2018. Geometallurgy—A route to more resilient mine operations. *Minerals*, vol. 8, no. 12, pp. 560. https://doi.org/10.3390/min8120560

Draper, N.R., Smith, H. 1998. Applied regression analysis vol. 326. John Wiley and Sons.

Elliott, R., and Barati, M. (2020). A review of the beneficiation of low-grade manganese ores by magnetic separation. *Canadian Metallurgical Quarterly*, vol. 59, no. 1, pp. 1–16. https://doi.org/10.1080/00084433.2020.1711654

Gutzmer, J., Beukes, N.J. 1996. Karst-hosted freshwater Paleoproterozoic manganese deposits, Postmasburg, South Africa. *Economic Geology*, vol. 91, no. 8, pp. 1435–1454. https://doi.org/10.2113/gsecongeo.91.8.1435

Habashi, F. 2008. Alloys: preparation, properties, applications. John Wiley and Sons. Hall, A.L. (1926). The manganese deposits near Postmasburg, west of Kimberley. *Transactions of the Geological Society of South Africa*, no. 29, pp. 17–66.

Hunt, J., Kojovic, T., Berry, R. 2013. Estimating comminution indices from ore mineralogy, chemistry and drill core logging. *University of Tasmania. Conference contribution*. https://hdl.handle.net/102.100.100/524994

Koch, P.H., Lund, C., Rosenkranz, J. 2019. Automated drill core mineralogical characterization method for texture classification and modal mineralogy estimation for geometallurgy. Minerals Engineering, no. 136, pp. 99-109. https://doi.org/10.1016/j.mineng.2019.03.008

Lamberg, P. 2011. Particles - the bridge between geology and metallurgy. Conference in Minerals Engineering: Luleå, 8-9 February 2011. Presented at the Konferens i mineralteknik 2011: 08/02/2011 - 09/02/2011. Retrieved from https://urn.kb.se/resolve?urn=urn:nbn:se:ltu:diva-40210

Lishchuk, V., Lamberg, P., Lund, C. 2015. Classification of geometallurgical programs based on approach and purpose. Presented at the SGA 2015 : 24/08/2015 - 27/08/2015. Retrieved from https://urn.kb.se/resolve?urn=urn:nbn:se:ltu:diva-33109

Lishchuk, V. 2016. Geometallurgical programs – critical evaluation of applied methods and techniques (Licentiate dissertation, Luleå tekniska universitet). https://orcid.org/0000-0002-9227-2470

Lund, C. 2013. Mineralogical, chemical, and textural characterisation of the Malmberget iron ore deposit for a geometallurgical model (Doctoral dissertation, Luleå tekniska universitet).

Lundberg, S.M., Lee, S.I. 2017. A unified approach to interpreting model predictions. *Advances in neural information processing systems*, 30. https://doi.org/10.48550/arXiv.1705.07874

Nagelkerke, N.J.D. 1991. A note on a general definition of the coefficient of determination. Biometrika, vol. 78, (no. 3), pp. 691–692.

Napier-Munn, T. 2018. The dense medium cyclone–past, present and future. *Minerals Engineering*, vol 116, pp. 107–113. https://doi.org/10.1016/j.mineng.2017.10.002

Parian, M. 2017. Development of a geometallurgical framework for iron ores-A mineralogical approach to particle-based modeling (Doctoral dissertation, Luleå University of Technology).

Smith, A.J., Beukes, N.J. 2016. Palaeoproterozoic banded iron formation hosted high-grade hematite iron ore deposits of the Transvaal Supergroup, South Africa. Episodes, vol. 39, no. 2, pp. 269–284. http://dx.doi.org/10.18814/epiiugs/2016/v39i2/95778

Song, J., Wang, H., Zuo, Y., Zhang, K., Yang, T., Yang, Y., Gao, C., Chen, T., Feng, G., Jiang, Z., Xiao, W. 2023. Building better full manganese-based cathode materials for next-generation lithium-ion batteries. *Electrochemical Energy Reviews*, vol. 6, no. 1, pp. 20. https://doi.org/10.1007/s41918-023-00184-8

Sun, X., Hao, H., Liu, Z., Zhao, F. 2020. Insights into the global flow pattern of manganese. *Resources Policy*, vol. 65, pp. 101578. https://doi.org/10.1016/j.resourpol.2019.101578

Sun, J., Dang, W., Wang, F., Nie, H., Wei, X., Li, P., Zhang, S., Feng, Y., Li, F. 2023. Prediction of TOC content in organic-rich shale using machine learning algorithms: Comparative study of random forest, support vector machine, and XGBoost. *Energies*, vol. 16, no. 10, pp. 4159. https://doi.org/10.3390/en16104159

Tsikos, H., Beukes, N.J., Moore, J.M., Harris, C. 2003. Deposition, diagenesis, and secondary enrichment of metals in the Paleoproterozoic Hotazel Iron Formation, Kalahari manganese field, South Africa. *Economic Geology*, vol. 98, no. 7, pp. 1449-1462. https://doi.org/10.2113/gsecongeo.98.7.1449.

Tusa, L., Frenzel, M., Pereira, L., Thiele, S., Tolosana-Delgado, R., and Gutzmer, J. (2025). Geometallurgy: Future Directions. *SEG Discovery*, no. 140, pp. 27–39. https://doi.org/10.5382/Geo-and-Mining-26.

Von der Heyden, B.P., Smith, A.J.B., Tsikos, H., Tadie, M., Mhlanga, X., Van Eeden, L., Backeberg, N., Schultz, T.G., Djeutchou, C. 2024. Manganese in South Africa: its mineral economics, geology and geometallurgy. South African Journal of Geology, vol. 127, no. 4, pp. 765–796. https://doi.org/10.25131/sajg.127.0039

Warke, M.R. 2016. Stratigraphic and geochemical framework of the Palaeoproterozoic rise in atmospheric oxygen: Transvaal supergroup (South Africa). PhD thesis, *The University of Manchester*.

Wills, B.A., Finch, J. 2015. Wills' mineral processing technology: an introduction to the practical aspects of ore treatment and mineral recovery. *Butterworth-heinemann*.

Willmott, C.J., Matsuura, K. 2005. Advantages of the mean absolute error (MAE) over the root mean square error (RMSE) in assessing average model performance. Climate Research, vol. 30, no. 1, pp. 79–82. https://doi.org/10.3354/cr030079 ➤



SOUTHERN AFRICAN MINE WATER CONFERENCE 2026

LET'S CONNECT

VENUE – GLENBURN LODGE AND SPA, MULDERSDRIFT
15 NOVEMBER 2026 – TECHNICAL WORKSHOPS
16 -17 NOVEMBER 2026 – TECHNICAL CONFERENCE
18 NOVEMBER 2026 – TECHNICAL VISIT

In Partnership:

ECSA and SACNASP Validated CPD Activity Credits = 0.1 per hour attended

SAIMM THE SOUTHERN AFRICAN INSTITUTE OF MINING AND METALLURGY

ABOUT THE CONFERENCE

The Southern African Institute of Mining and Metallurgy (SAIMM), in collaboration with the International Mine Water Association (IMWA), the Mine Water Division of the Water Institute of Southern Africa (WISA-MWD) and Mintek, warmly invites you to the Southern African Mine Water Conference 2026, a premier gathering where science, technology and sustainability intersect.

Guided by the theme "Let's Connect," this conference is more than an event – it's a movement to bridge disciplines, foster innovation and build resilient solutions for mine water management. Attendees will explore a wide spectrum of topics, from the complexity of mine water geochemistry to the transformative power of AI-driven modelling and simulation.

Discover how mining-influenced water (MIW) can be repurposed through circularity and value recovery and gain insights into the latest advancements in water treatment technologies and microbial processes that are reshaping environmental stewardship.

Whether you are a researcher, engineer, policymaker or industry practitioner, this is your chance to engage with cutting-edge developments, share your expertise and help shape a more connected future for mine water innovation.

CONFERENCE TOPICS

Explore cutting-edge developments and share insights on:

- Mine water geochemistry
- Utilisation of mining-influenced water (MIW), circularity and recovery of value products
- Modelling and simulation
- Artificial Intelligence applications
- Water treatment technologies
- Microbial processes in mine water systems

CALL FOR PAPERS/ PRESENTATIONS

Prospective authors are invited to submit short abstracts of not more than 500 words. Abstracts should consist of 4 paragraphs describing the presentation's relevance, the methods used, the key results and their application as well as implications.

Authors of accepted abstracts will be required to submit a full paper for peer review and publication in the conference proceedings. A presentation only option will be considered.

KEY DATES

21 May 2026 – Submission of abstracts
27 June 2026 – Submission of papers

SUBMIT AN ABSTRACT

FOR FURTHER INFORMATION, CONTACT:

Gugu Charlie,
Conferences and Events Coordinator

E-mail: gugu@saimm.co.za
Tel: +27 11 530 0238
Web: www.saimm.co.za